Pflügers Arch – Eur J Physiol (1996) 432:1080–1090

INSTRUMENTS AND TECHNIQUES

L. John Greenfield Jr · Robert L. Macdonald

Whole-cell and single-channel $\alpha_1\ \beta_1\ \gamma_{2S}$ $GABA_A$ receptor currents elicited by a "multipuffer" drug application device

Received: 29 April 1996 / Received after revision: 10 June 1996 / Accepted: 11 June 1996

Abstract Pharmacological characterization of ion channels and receptors in cultured neurons or transfected cell lines requires microapplication of multiple drug solutions during electrophysiological recording. An ideal device could apply a large number of solutions to a limited area with rapid arrival and removal of drug solutions. We describe a novel "multipuffer" rapid application device, based on a modified T-tube with a nozzle made from a glass micropipette tip. Drug solutions are drawn via suction from open reservoirs mounted above the recording chamber through the device into a waste trap. Closure of a solenoid valve between the device and the waste trap causes flow of drug solution though the T-tube nozzle. Any number of drug solutions can be applied with rapid onset (50–100 ms) after a brief fixed delay (100–200 ms). Recombinant $\alpha_1\beta_1\gamma_{2S}$ $GABA_A$ receptors (GABARs) transfected into L929 fibroblasts were recorded using whole-cell and single-channel configurations. Application of GABA resulted in chloride currents with an EC_{50} of 12.2 μM and a Hill slope of 1.27, suggesting more than one binding site for GABA. GABAR currents were enhanced by diazepam and pentobarbital and inhibited by bicuculline and picrotoxin. Single-channel recordings revealed a main conductance state of 26–28 pS. This device is particularly suitable for rapid, spatially controlled drug applications onto neurons or other cells recorded in the whole-cell configuration, but is also appropriate for isolated single-channel or multichannel membrane patch recordings.

Key words Drug application · Superfusion · $GABA_A$ receptor · Ion channel · Electrophysiology · Pharmacological technique

L.J. Greenfield Jr (✉)
Departments of Neurology, Neuroscience Laboratory Building, 1103 E. Huron, Ann Arbor MI 48904-1687, USA

R.L. Macdonald
Department of Neurology and Physiology, University of Michigan Medical Center, Michigan, USA

Introduction

Microapplication of drug solutions to cells in culture during electrophysiological recording has been a vexing problem for neurophysiologists. An ideal drug application system would provide rapid onset of solution change, instantaneous shift to a constant drug concentration, rapid washout of drug after application, no additional superfusion or drain requirements and an unlimited ability to change solutions. Pressure ejection of drug solutions from single or multibarrel pipettes pulled to small tip openings (10–20 μm) can rapidly deliver a drug solution to a localized area, but this technique is limited to application of a single drug concentration per pipette barrel. More recently, the U-tube or T-tube approach has been used to apply multiple drug concentrations [22]. In this system, fluid is sucked through a U-shaped tube past a small opening (or perpendicular "T"-tube) until flow is is abruptly terminated by closure of a solenoid valve. Fluid is then forced out the U-tube or T-tube opening by gravity. Advantages of this system include relatively fast onset of solution changes and delivery of a uniform drug concentration, as well as potentially unlimited drug concentrations. Disadvantages include the inability to apply drugs to a limited region of the dish (to minimize desensitization of receptors on other cells), and the larger volume of applied drug requires simultaneous superfusion with saline and a drain system, which may add noise to the recording.

To address these problems, we have developed a novel device, the "multipuffer", which combines the tip of a glass puffer pipette (allowing precise control of the location and volume of application) with a T-tube (for rapid uniform drug concentration). Addition of the puffer tip reduces the superfused volume and allows precise control of location, but lengthens the delay between solenoid closure and drug application. The "T-tube" is incorporated into an acrylic holder fitted with a metal tube over which a glass micropipette tip is fitted and secured with an O-ring. Application of drug thus occurs through the fine tip of a glass micropipette. This device allows any number of drug solutions to be applied though the same

pipette tip to a small area of a culture dish with fairly rapid solution exchange. This enables the experimenter to apply a whole range of drug solutions or concentrations during an experiment, and to change or add drug concentrations during a recording. The tip of the device can be placed very close to the cell or patch of interest, and need not be removed between applications. As the position of the device does not change during a recording, drug applications are more accurate and consistent. Drug solutions are "washed away" by the sucking action of the device between applications of drug, which minimizes problems of drug desensitization. The small volume of solution applied obviates the need for simultaneous superfusion and drainage systems, and the ability to cycle quickly among multiple drugs, in any order, makes each experiment more likely to yield useful data.

We have used this device to characterize the whole-cell and single-channel pharmacology of recombinant $GABA_A$ receptors (GABARs) in transfected L929 cells [4, 9, 15, 16, 27], native GABARs in cortical neurons in primary culture [14], and in acutely isolated hippocampal dentate granule cells [13]. In this study, we examined the kinetics of the drug application system and the resulting effects on recombinant GABAR currents.

Materials and methods

Multipuffer drug application system

The multipuffer application device consists of a "head piece" made from a length of 9.53 mm (3/8″) diameter acrylic rod, with the "U-tube" solution passage drilled into the block (see Fig. 1A). The "cross tube" (i.e., the bottom of the "U") must be drilled through the side of the block and the opening plugged with a glued insert. The front end of this head piece is drilled with recesses for the back end of the pipette tip and the O-ring that secures it. A fine hole is drilled through the center of the pipette recess into the "cross tube" of the U-tube, and a piece of steel tubing is pressed or glued into this hole. The O-ring and pipette tip are secured with an acrylic cap that screws over the headpiece, tightening down on the O-ring to form an air-water-tight seal and to secure the pipette tip in place. The back end of the head piece has stainless steel tubes inserted into the U-tube holes for attaching polyethylene tubing (Intramedic PE 190, Clay Adams, Persippany, N.J., USA). The head piece is held by a rigid plastic tube that is attached to a micromanipulator (eg. Brinkman, Leitz, etc.). The polyethylene tubing from the head piece passes out the open end of the plastic support tube and is connected to the valve manifold (the source of drug solutions) and to the solenoid valve, which in turn is connected to the vacuum flask. A short length of compressible (eg. Tygon) tubing is used to make these connections, so that a pressure clamp can be used to stop the flow of drug solutions when appropriate.

Drugs solutions are stored in open plastic (Corning or Falcon) or glass (Pyrex) 50-ml tubes in a test tube rack suspended on a ringstand at a fixed height above the microscope stage (generally 20–40 cm depending on the rate of flow desired). Four polyethylene "feed" tubes (PE 190) pass from the open drug reservoirs to a manifold (Hamilton HV PD4-5 manual valve) to select which drug solution flows to the device. Feed tubes can be moved from one solution to the next by hand, obviating the need for a valve position for each solution. The "drain end" of the multipuffer tubing is connected to a solenoid valve [General Valve 3 way 12 V Teflon membrane valve no. 1–17–900 or Cole Parmer (Niles, Ill., USA) CP no. 01367–72, mounted in "normally open" configuration]. The solenoid valve is actuated by a Valve Driver II (General Valve, Fairfield, N.J., USA) controlled by a Repeat Cycle Timer (Lafayette Instrument, Lafayette, Ind., USA). Nominal closing time for these valves is 8–15 ms. The solenoid valve is then connected to a vacuum pump [e.g., modified "Supra" or larger fish tank pump (Second Nature)] or other source of vacuum via a solution trap (1- to 2-l vacuum flask). While we have minimized costs by using a manual switching valve and a standard interval timer, more elaborate control could be achieved by using a computer to control both an electronic mechanized manifold valve and the solenoid. The configuration of the drug reservoirs, manifold, multipuffer device, solenoid, and vacuum trap is shown in Fig. 1B. Placement flexibility is greatest when the device is used with an inverted microscope.

A critical element in the function of the device is the glass pipette tip. We have used Pyrex glass tubes (Drummond Custom Glass N-51-A) with inside diameter (I.D.) of 0.6 mm and outside diameter (O.D.) of 1.2 mm, pulled to a tip diameter of 30–70 μm using a P-87 Flaming Brown Microelectrode Puller (Sutter Instrument). The type of glass is unimportant, though microelectrode glass with an internal glass filament should not be used, as the filament tends to fracture when placed on the holder and the glass fragments can plug the tip or be sucked back to the solenoid where they can puncture the Teflon membrane of the valve. The distal 1 cm or so of the pulled pipette tip can be broken cleanly from the remainder of the electrode shaft after scoring with a diamond pen. The tip is then placed on the assembled holder and pushed through the O-ring and the screw cap tightened to hold the tip in place. It is essential to cut the tip off at a length long enough to have the open end well seated in the device and clamped by the O-ring, but short enough that the metal insert comes to the beginning of the tip taper.

When a drug is to be applied, the appropriate feed tube is selected with the 4:1 manifold valve. After 5–10 s (to allow the drug solution to pass into the multipuffer), the solenoid is activated for a predetermined interval. When the solenoid valve closes, the vacuum stops and solution flows via gravity from the drug reservoir out the multipuffer tip onto the region of interest. The rate of solution application and the delay between solenoid activation and arrival of drug depend directly on the diameter of the glass pipette tip. Pipettes pulled to a internal tip diameter of about 50–70 μm allow fast enough flow to give onsets within 100–200 ms of solenoid closure without "blowing away" the cell or patch (see Fig. 2). Smaller openings give more spatially controlled applications but longer onset delays and increased mixing of drug with saline from the recording bath.

Under most experimental conditions with tip configurations used, the rates of solution flow are well below those normally associated with generation of turbulence. The onset of turbulent flow can be predicted by the Reynold number, R_N, given by the equation:

$$R_N = 2\rho a u/\eta \quad (1)$$

where ρ is the fluid density, u is the linear fluid velocity, a is the radius of the capillary tube, and η is the viscosity (in $g \cdot m^{-1} \cdot s^{-1}$, or Poise, where 1 cp = 1 mNs/m^2). Onset of turbulence is generally associated with an R_N greater than 2000. The values of ρ and η for a dilute solution can be approximated by those for water (ρ = 1.00 g/cm^3, η = 1.009 cP ≈0.01 $g \cdot cm^{-1} \cdot s^{-1}$), while the linear velocity can be determined from the delay between solenoid actuation and solution change, since the applied solution travels a fixed distance down the length of the T-tube to the electrode tip. For a delay of 100 ms (seen with application of a KCl solution to an "open" electrode through a glass capillary tip opening of 60 μm diameter) and a travel distance of 1.0 cm, the velocity would be 10 cm/s. The calculation of R_N is thus:

$$R_N = 2 \cdot (1.00\ g \cdot cm^{-3}) \cdot (3 \cdot 10^{-3}\ cm) \cdot (10\ cm \cdot s^{-1}) / (0.01\ g \cdot cm^{-1} \cdot s^{-1}) = 6 \quad (2)$$

This calculation implies that flow rates commonly used with this application device are far below those associated with the onset of turbulence, and could probably be increased 100-fold (e.g., by application of pressure) without inducing flow-related turbulence.

Test applications with fast green dye dissolved in water can be delivered either into a test dish or the actual recording chamber under direct microscopic observation to ensure that flow is present

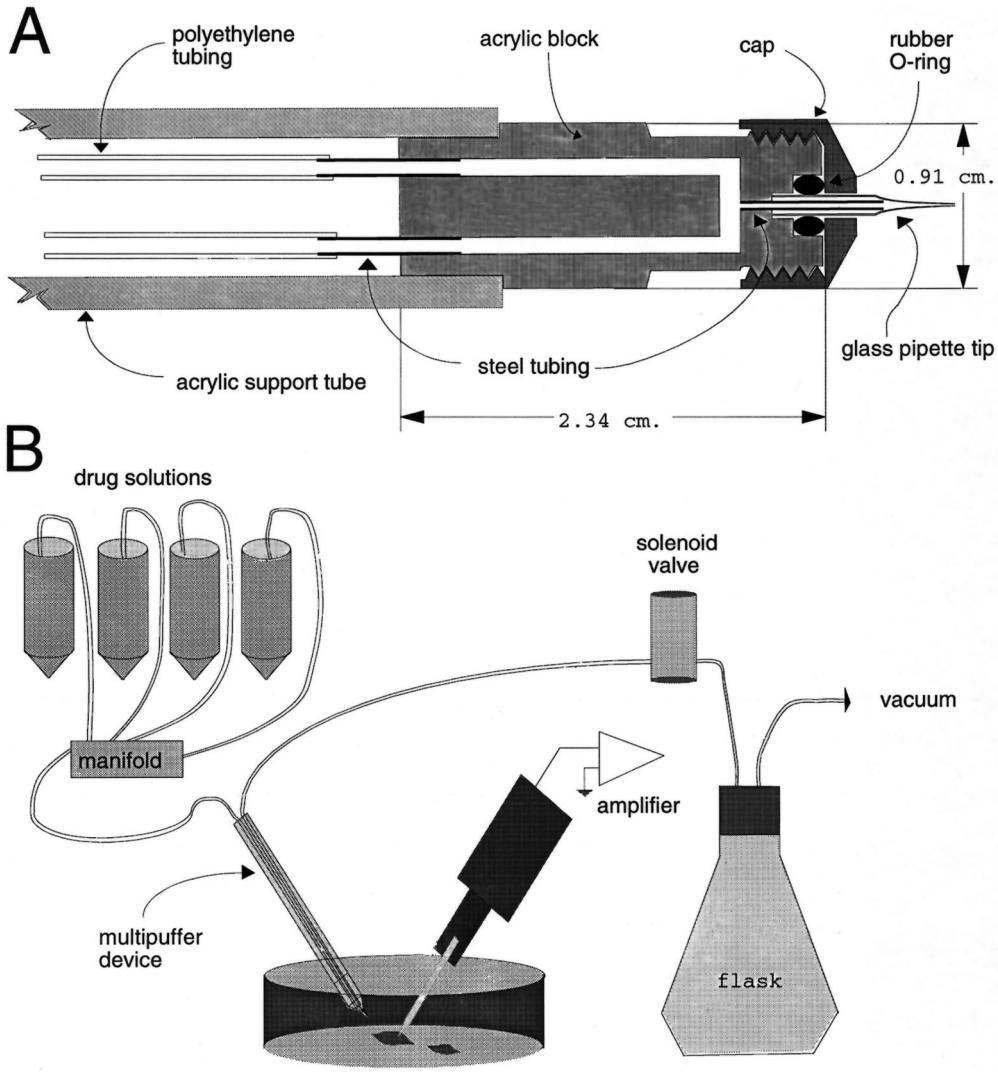

Fig. 1 **A** Schematic of the multipuffer U-tube device. **B** Simplified plan of a recording set-up including a multipuffer for drug application. See Materials and methods for details of implementation

prior to starting the experiment. This will give a good measure of the force and speed of drug application and the duration of the fixed delay, and ensures that there are no plugs or leaks. Air leaks around the pipette tip appear as bubbles between the device and the solenoid, which significantly slow the application by destroying the "water hammer" created by the solenoid. Bubbles elsewhere are less problematic but can inhibit the rapid change of drug solutions.

The dye trial also shows how long it takes to clear a drug solution from the line. Depending on the lengths of tubing involved, the flow of drug should be started about 10 s prior to application and allowed to continue for 5–10 s after the solenoid reopens. To wash out any residual drug and to maintain constant flow of fluid without wasting drug/saline solutions, we let distilled water flow through the apparatus at other times. The constant suction from the dish (due to the Bernoulli effect) ensures that no water enters the recording bath solution, though enough time must be allowed for drug to fill the line prior to drug application. Alternatively, the tubing can be charged with saline and both drain and source tubes can be clamped shut between drug applications (so there is no drainage of solution from the dish).

Cell culture and transfection

Mouse L929 cells (American Type Culture Collection, Rockville, Md., USA) were grown in Dulbecco's modified Eagle's medium (DMEM) with 10% horse serum and 100IU/ml penicillin and 100 μg/ml streptomycin at 37°C in 5% CO_2/95% air. Full-length cDNAs encoding bovine α_1, β_1 and γ_{2S} [28] subcloned individually into pCMVneo expression vectors, and the cDNA encoding *Aequorea victoria* green fluorescent protein (*gfp*, generously provided by Dr. Martin Chalfie) [3], subcloned into pCMVneo as a marker of transfection were transfected into L929 cells in a ratio of 1:1:1:3 (3 μg of each of the GABAR subunits and 9 μg of pCMV-*gfp*), as previously described [2]. A total of 18 μg of DNA was added per 60-mm dish in 0.5 ml of transfection buffer. Cells were incubated for 4–6 hours in 3% CO_2 at 37°C and then shocked for 30 s with 50% glycerol/transfection buffer solution. The following day, transfected cells were treated with DNase I, and replated onto gridded 35-mm plates (Mecanex) for subsequent identification during scoring and electrophysiological recording. Using fluorescence micrography with fluorescein filters (Chroma High-Q FITC, no. 41012, excitation 460–500 nm, emission 510 nm long pass), the positions of positive cells on the grid were drawn for subsequent electrophysiological recording within 48–60 h after transfection [2].

Electrophysiological recording

Prior to recording, the DMEM medium was replaced with multiple washings of external recording medium containing (in mM): 142

NaCl, 8.1 KCl, 6 $MgCl_2$, 10 glucose, 10 4-(2-hydroxyethyl)-1-piperazineethanesulfonic acid (HEPES) (pH 7.4). Recording pipettes contained (in mM): 153 KCl, 1 $MgCl_2$, 5 ethylenebis(oxonitrilo)tetraacetate (EGTA) and 10 HEPES (pH 7.3). These solutions produce a Cl^- equilibrium potential (E_{Cl}) of approximately 0 mV and a K^+ equilibrium potential (E_K) of –75 mV. To quantify the response time of the drug application system, increasing concentrations of K^+ were made by serial dilution of the recording medium with 158 mM KCl, without changing solution osmolality. Solutions with increasing K^+ concentration were applied to an "open electrode" recording in constant-current mode to record the change in electrode tip potential. Most $GABA_A$ receptor experiments were performed in the whole-cell configuration in voltage-clamp mode at –75mV using an Axopatch 200A amplifier. Whole-cell currents were filtered at 2 kHz and digitized on line by a Labmaster Tl-40 ADC at 200 Hz and recorded using Axotape 2.0 software (Axon Instruments). Peak currents were measured from digitized records. For single-channel recordings, "outside-out" patches were formed using standard techniques [10]. Single-channel currents were digitized on-line at 20 kHz using Axotape 2.0 software and later analyzed using IPROC (Axon Instruments), PRISM (Graphpad) and software developed in our laboratory [19]. All chemicals and drugs were obtained from Sigma.

Results

Response time course for multipuffer application

Prior to recording receptor-elicited currents, we wished to quantify the rate of solution change and the delay between solenoid actuation and solution change. To eliminate the role of membrane capacitance, we measured the change in potential of an open electrode tip (recorded in current-clamp mode, with standard intracellular pipette solution, see Materials and methods) in response to a step change in K^+ concentration from that of the extracellular recording medium (8 mM) to 158 mM KCl, the maximum K^+ concentration possible without changing solution osmolality. The time course of the rising phase of a step change from 8 mM to 158 mM K^+ is shown in Fig. 2A. The 10% to 90% rise time in this case was 57.4 ms (mean ± SEM = 54.4±4.96 ms, n = 5, see Table 1). The time for a "complete" transition (at least 98% of the maximal voltage change) was 101.4±9.4 ms (n = 5), which reflects the time required for a complete solution change. The time course of the electrode tip potential change was well fit with a single exponential decay with a time constant, τ, (defined as 1–1/e of the complete transition time) of 23±3 ms (n = 5). The delay from the onset of solenoid closure to the onset of the voltage change at the electrode tip was very consistent (118±3.3 ms). On a slower time scale (Fig. 2B), the square shape of this voltage response indicated that the K^+ concentration and flow characteristics remained fairly constant during the application. The stability of the plateau response implied an adequate "concentration clamp" of the perfused region. Time characteristics of the falling phase of the K^+ step application are also given in Table 1; however, these should be viewed as "best case" characteristics for brief (2–3 s) applications. With longer applications, the applied drug may accumulate in the medium and diluted drug will wash past the cell or patch when the application ends, making the time course of the concentration change indeterminate.

Although the ion gradient at the electrode tip was not restricted by a membrane (and hence not predicted by the Nernst equation), the magnitude of this potential

Table 1 Rise and fall time characteristics of multipuffer application. (n = 5)

Variable	Rising phase		Falling phase	
	Mean	SEM	Mean	SEM
Delay (ms)	118.1	3.33	93.7	7.1
Amplitude (mV)	3.09	0.05	3.43	0.05
Transition time (ms)	101.4	9.4	136.3	6.29
Rise time (10–90%)	54.4	4.96	75.5	54.7
τ [= (1–1/e) · rise time]	23.0	2.98	54.7	3.09

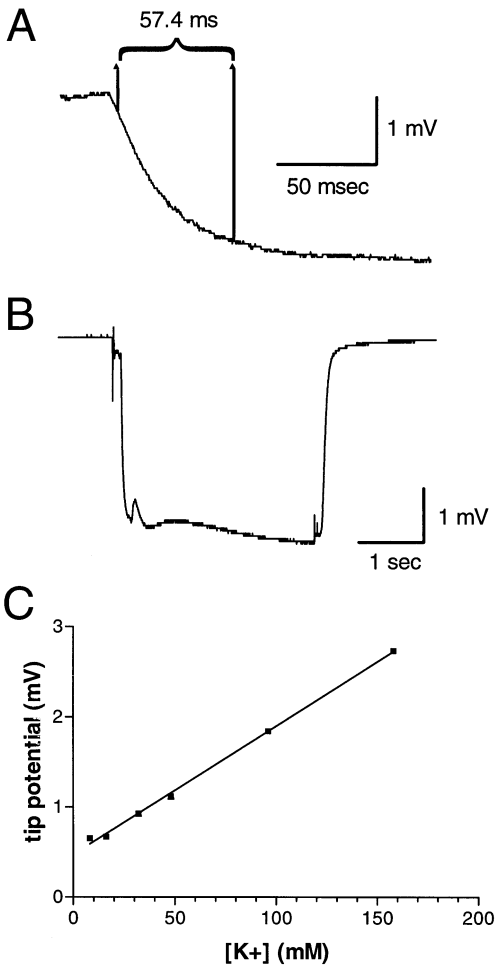

Fig. 2A–C Voltage responses of an open electrode tip to application of solutions containing different concentrations of K^+. **A** Time course of the rising phase of a step change from 8 mM to 158 mM K^+. The 10% to 90% rise time was 57.4 ms. **B** Voltage response to a pulse step change from 8 mM to 158 mM K^+ on a slower time scale. The "*square*" shape of this response indicates that the K^+ concentration remained fairly constant during the application. **C** Plot of the amplitude of the voltage response of an open electrode to increasing concentrations of K^+. Each *point* represents the mean of three responses; SEM *error bars* fall within the *symbol diameter*

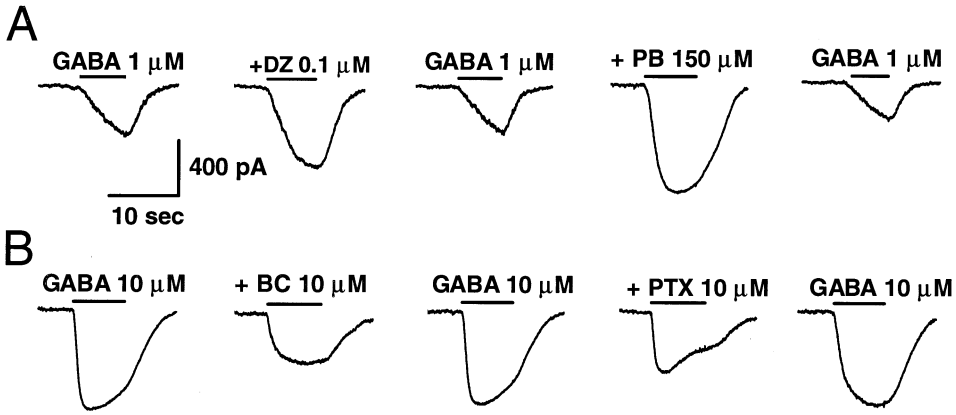

Fig. 3A, B Whole-cell currents in L929 cells transfected with bovine $\alpha_1\beta_1\gamma_{2S}$ $GABA_A$ receptor cDNAs elicited by GABA and pharmacological agents. **A** Currents elicited by GABA (1 μM) alone (*1st.*, *3rd* and *5th traces*) or in the presence of diazepam (*DZ*, 0.1 μM, *2nd trace*) or pentobarbital (*PB*, 150 μM, *4th trace*). **B** Currents elicited by GABA (10 μM) alone (*1st*, *3rd* and *5th traces*) or in the presence of bicuculline (*BC*, 10 mM, *2nd trace*) or picrotoxin (*PTX*, 10 mM, *4th trace*). All currents were recorded in the whole-cell configuration at –75 mV.

should be a function of K^+ concentration. Solutions with varying K^+ concentrations were made by diluting the 158 mM KCl stock solution with the extracellular recording medium, yielding K^+ concentrations of 8, 16, 32, 48, 96, and 158 mM, with constant osmolality. Peak voltage responses for each K^+ concentration are plotted in Fig. 2C. Although these potential shifts were small (maximum 3.09±0.05 mV for the 158 mM KCl solution) and there was a flow-related voltage offset of 0.64 mV, the amplitude of the tip potential varied linearly with K^+ concentration (slope of 14.2 μV/mM K^+, r = 0.996).

Whole cell $GABA_A$ receptor currents

Next we wished to determine whether the multipuffer device was useful in characterizing the pharmacological properties of recombinant $GABA_A$ receptor (GABAR) currents. Whole cell currents were recorded from L929 cells 48 h after transfection with $\alpha_1\beta_1\gamma_{2S}$ GABAR cDNAs. Due to the symmetrical Cl^- concentrations inside and outside the cell (after exchange of intracellular ions with the pipette medium), GABAR currents were inward (downward) when the cell was voltage-clamped at –75 mV. Currents elicited by GABA (1 μM, Fig. 3A,

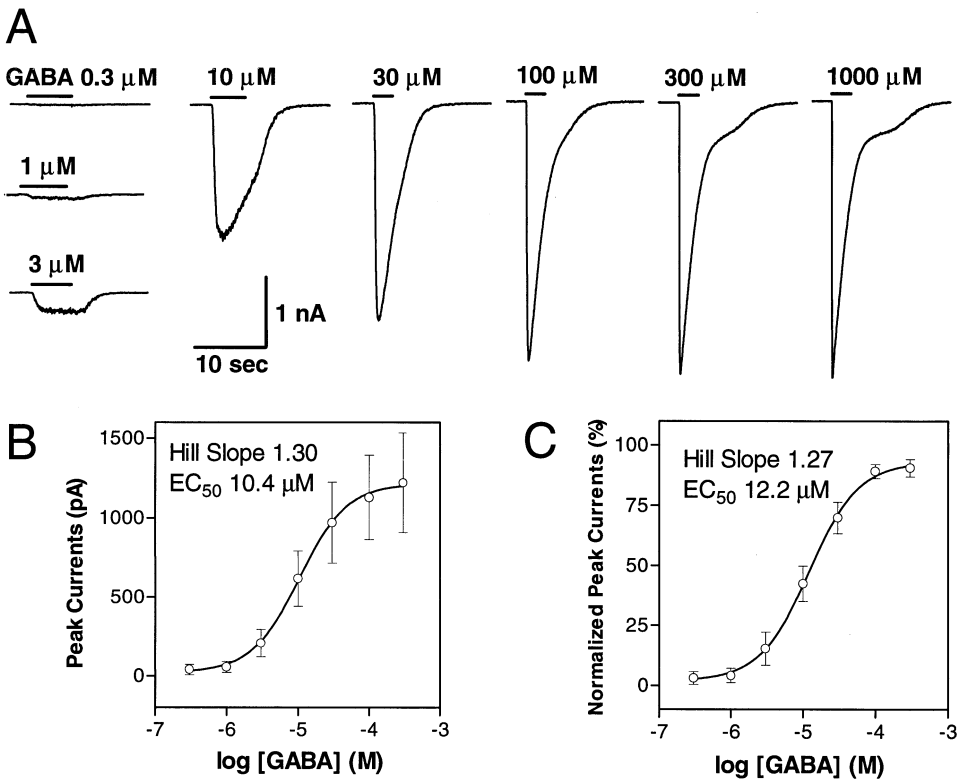

Fig. 4A, B Concentration/response relationship for L929 cells transfected with $\alpha_1\beta_1\gamma_{2S}$ $GABA_A$ receptor cDNAs. Whole-cell recordings were carried out at –75 mV. **A** Sequential applications of increasing concentrations of *GABA* revealed threshold currents at 1 μM GABA and saturating currents at 100 μM GABA. **B** A plot of peak currents versus GABA concentration reveals an EC_{50} of 10.4 μM (n = 13) and a Hill slope of 1.30. **C** A plot of normalized peak currents versus GABA concentration shows no change in EC_{50} (12.2 μM) or Hill slope (1.27)

traces 1, 3 and 5) were enhanced by the coapplication of diazepam (DZ, 0.1 μM, second trace) or pentobarbital (PB, 150 μM, fourth trace), as expected for receptors containing these subunits [17]. Similarly, currents elicited by GABA (10 μM, Fig. 3C, traces 1, 3 and 5) were inhibited by bicuculline (BC, 10 μM, second trace), a competitive antagonist at the GABA-binding site, or by picrotoxin (PTX, 10 μM, fourth trace), a non-competitive GABAR antagonist [23, 24, 30].

Sequential applications of increasing concentrations of GABA (Fig. 4A) during whole-cell recordings revealed threshold currents at approximately 1 μM GABA and saturating currents at 100 μM GABA. A plot of peak currents versus GABA concentration revealed an EC_{50} of 10.4 μM (Fig. 4B, n = 13), with increasing variability of amplitude at larger GABA concentrations due to the variable maximal current amplitude (hence variable number of GABAR channels expressed) in each cell. When the responses of each cell were normalized to the maximal peak current (at any concentration) for that cell (Fig. 4C), the variability of maximal amplitude was eliminated, while the EC_{50} was virtually unchanged (12.2 μM). For both actual and normalized peak current concentration/response curves, there was a Hill slope greater than 1.0 (1.30 for actual currents, 1.27 for normalized data), suggesting that more than one GABA-binding site with positive cooperativity may be involved in channel opening.

Activation and desensitization of GABAR currents

The validity of the concentration/response relationship to GABA may depend on how rapidly the currents are activated by the arrival of GABA-containing solutions; if this arrival is gradual, significant desensitization may occur and the peak response may be blunted [5]. To assess the rates of activation and desensitization for these receptors, we initially examined the time course of onset of GABAR currents for a single cell (Fig. 5). In Fig. 5A, currents elicited by increasing concentrations of GABA were aligned at the time point of solenoid closure. As GABA concentration increased, the slope of current onset increased, with an initial delay and an "S-shaped" initial rising phase. These same responses were normalized to the maximal current and then plotted on an expanded time scale (Fig. 5B). Since the distance from the T-tube outlet and the cell was constant, the relatively longer delays before the onset of current at lower GABA concentrations and the sigmoidal shape of current onset appear to be a function of receptor activation, and likely reflect the combination of GABA association and dissociation rates, cooperativity between GABA-binding sites, and channel opening rates (see below). At GABA concentrations up to 300 μM, the onset of GABA currents was significantly slower than the rise time for the stepped KCl gradient to an open electrode (leftmost trace, Fig. 5B), implying that the rate of solution application was not limiting for the development of current at

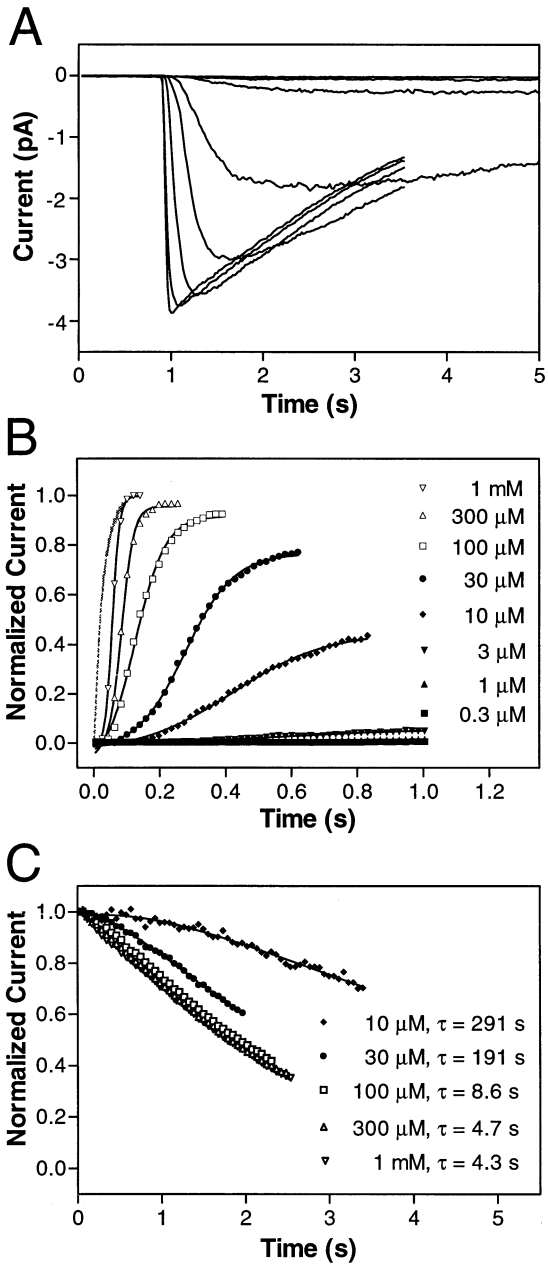

Fig. 5A–C Currents elicited by increasing concentrations of GABA in a single L929 fibroblast transfected with $\alpha_1\beta_1\gamma_{2S}$ $GABA_A$ receptor cDNAs. **A** Whole-cell currents, aligned at the time point of solenoid closure, showing an increased rate of onset and faster desensitization with increased GABA concentration. **B** The same responses normalized to the maximal current and plotted on an expanded time scale. *Symbols* for each concentration are noted in the figure. At GABA concentrations up to 1 mM, the onset of GABA currents was significantly slower than the rise time for the step KCl gradient to an open electrode (*leftmost trace*). **C** Early desensitization of the response at concentrations between 10 μM and 1 mM during continued application of GABA. Currents were normalized to the peak current for each concentration at the onset of desensitization. Desensitization was concentration dependent but approached a maximal rate at 100–300 μM. The time course of desensitization was modeled by a single exponential decay with time constants as noted in the figure

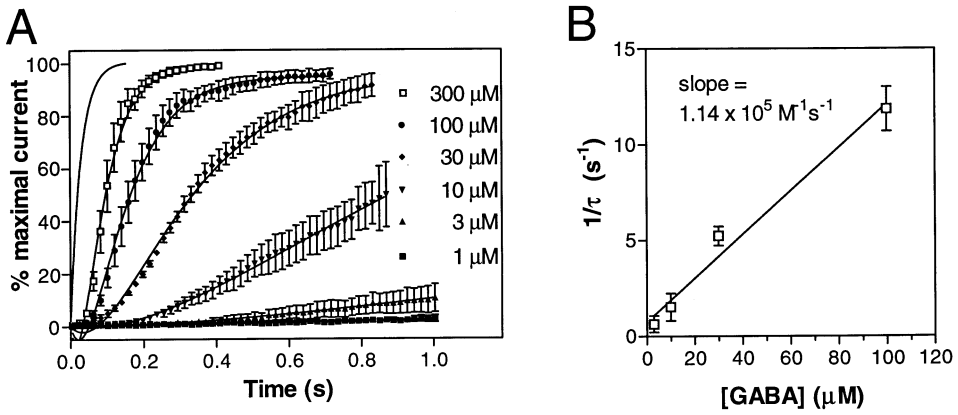

Fig. 6A, B Initial GABA receptor current development normalized to the maximal current for each cell (n = 5) at GABA concentrations ranging from 1 μM to 300 μM. *Symbols* for each concentration are noted in the figure. The initial phase of currents elicited by increasing concentrations of GABA was fit with the sum of two exponential association curves. **B** The exponential activation coefficients ($k_{act} = 1/\tau_1$) corresponding to the linear portion of the concentration/response relationship (3–100 μM) were plotted against GABA concentration. A linear relationship was observed with a slope of 1.14×10^5 M^{-1} s^{-1} (r^2 = 0.98), which estimates the minimum opening rate of the receptor as a function of GABA concentration

these concentrations. The time to peak for 1 mM GABA applications was approximately 75 ms (in this cell), somewhat less than the time for "complete" solution change for a K^+ gradient at an open electrode (101 ms) and approaching the 10–90% rise time (54 ms).

Early desensitization of the response was not observed at GABA concentrations below 10 μM (Fig. 5A). At concentrations between 10 μM and 1 mM, an early phase of desensitization during continued application of GABA was observed to occur in this cell. When normalized to the peak current obtained for each concentration at the onset of desensitization (Fig. 5C), current desensitization was concentration dependent but approached a maximal rate at 100–300 μM. The time course of desensitization could be adequately modeled by a single exponential decay with time constants varying from 4.3 s for 1 mM GABA to 290 s for 10 μM GABA. The rates of desensitization were highly variable among cells, however, and a detailed examination of desensitization time course was felt to be beyond the scope of the current study. We did not observe the rapid phases of desensitization (with time constants of the order of tens to several hundred milliseconds) seen with excised membrane patches and ultrarapid drug application techniques [5, 12].

We focused instead on the time course of onset of GABAR currents, which was more consistent among cells under these conditions. When normalized to the maximal current, the initial rate of development of GABAR currents was remarkably uniform at concentrations comprising the sigmoidal portion of the concentration/response curve (1–300 μM, Fig. 6A). With 1 mM GABA applications, the rate of current onset was faster than for 300 μM; however, the peak current amplitude was often smaller than at 100 or 300 μM, implying some desensitization of the response prior to the development of peak current. These currents were therefore not included in the evaluation of the initial time course. The time course of currents elicited by increasing concentrations of GABA, $I(t)$, could be fit with the sum of two exponential association curves, of the form $I(t) = A\cdot[1–\exp(–t/\tau_1)]–B\cdot[1–\exp(–t/\tau_2)]$. The second exponential component with a negative coefficient was necesary to account for the concentration-dependent delay and sigmoidal rise of the initial slope of the response, which was most obvious for the 10 μM applications (Fig. 6A). The exponential activation coefficients ($k_{act} = 1/\tau_1$) corresponding to the linear portion of the concentration/response relationship (from 3 μM to 100 μM) were directly proportional to the GABA concentration with a slope of 1.14×10^5 M^{-1} s^{-1} (r^2 = 0.98), providing a rough estimate of the minimum opening rate of the receptor as a function of GABA concentration (Fig. 6B).

Single channel $GABA_A$ receptor currents

To assess the utility of the multipuffer device for single-channel recordings, we recorded single-channel currents elicited by 1 μM GABA in outside-out patches (Fig. 7). Applications of increasing concentrations of GABA resulted in concentration-dependent increases in channel opening frequency and burst duration and, in multichannel patches (Fig. 7A), it increased the frequency of simultaneous openings of multiple channels. Kinetic analysis showed that single-channel currents from one such "outside-out" membrane patch demonstrated characteristics similar to those seen with this combination of subunit subtypes in prior recordings from this laboratory (1,24) using single-pipette GABA application, with a mean open time of 3.94 ms. Approximately 85% of openings occurred in bursts lasting an average of 10 ms with about two openings per burst (n = 277 openings). Figure 7B shows a sample tracing of single-channel currents elicited by GABA (1 μM) at multiple time scales to demonstrate the structure of burst openings. A histogram of current amplitudes for a small number of openings

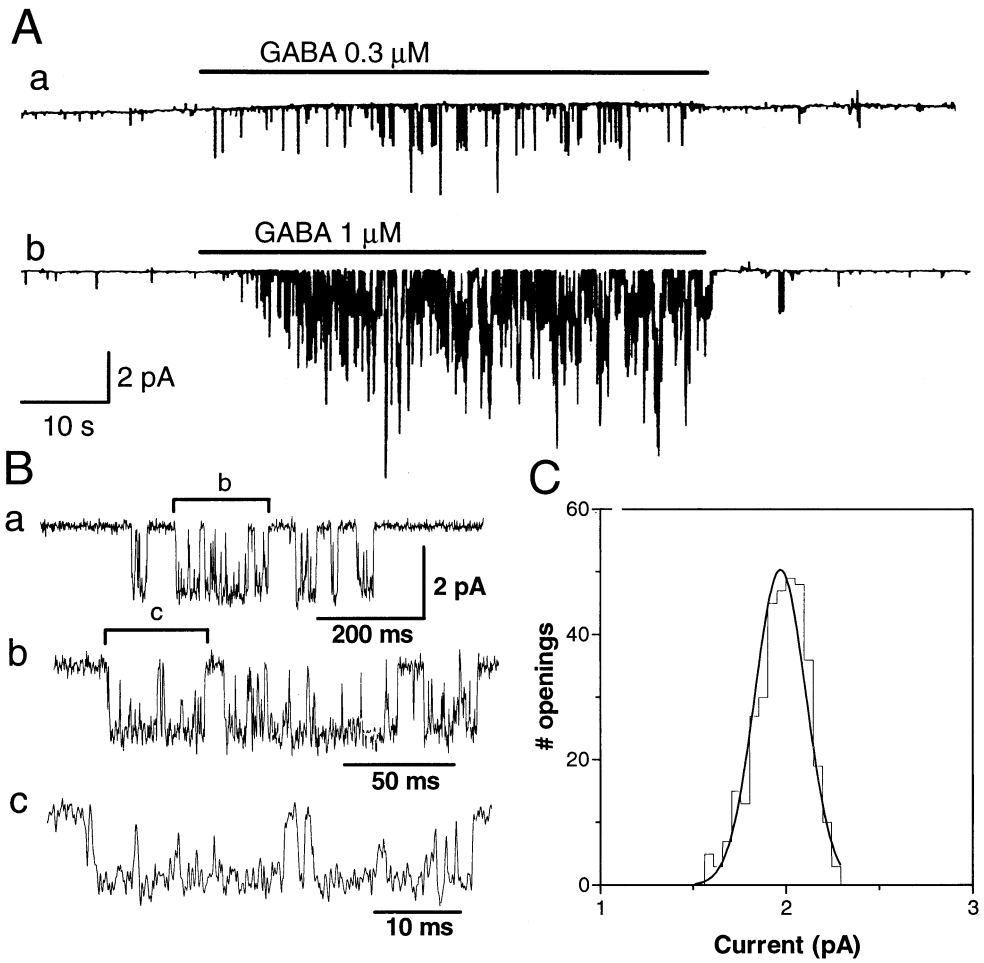

Fig. 7A, B Single-channel currents elicited by GABA (1 mM) in "outside-out" membrane patches from an L929 cell transfected with $\alpha_1 \beta_1 \gamma_{2S}$ GABA receptor subunits, voltage-clamped at –75 mV. **A** Prolonged application of 0.3 μM GABA (**a**) and 1 μM GABA (**b**) to an outside-out patch containing multiple channels (at least 4). **B** Current traces of single-channel openings of $\alpha_1 \beta_1 \gamma_{2S}$ channels at 3 time scales. *Traces* **b** and **c** are expanded segments from *traces* **a** and **b**, respectively. **C** Amplitude histogram of single-channel current amplitudes showing a single conductance state of 26 pS in bovine $\alpha_1 \beta_1 \gamma_{2S}$ channels

(Fig. 7C) shows a single main conductance state of approximately 26 pS.

Discussion

The whole-cell pharmacology and single-channel characteristics of $\alpha_1 \beta_1 \gamma_{2S}$ GABAR currents obtained using the multipuffer device were consistent with prior characterizations of this receptor isoform, measured in our laboratory using the single "puffer" pipette system [1], but use of the multipuffer system enabled a more complete pharmacological characterization to be performed for each cell or patch. The system was "quiet" enough to allow single-channel recordings at high amplifier gain (100 mV/pA). We did not analyze a large number of channel openings for detailed kinetics or the presence of subconductance states, as these have been studied in detail previously in our laboratory [1].

Application of KCl solutions to an open electrode demonstrated solution change with an exponential time constant, τ, of 27 ms and 10–90% rise time of 54 ms. Although this rise time was significantly faster than the rate of rise for the highest concentrations of GABA tested (1 mM), for the pharmacological data derived from this system to be meaningful, the rate of drug application must be fast enough to exceed the activation rate and minimize early desensitization of the receptor under study. With the advent of ultrarapid application devices [5, 12, 20, 21, 29], the results of the current study can be compared to those measured using techniques that offer improved kinetic resolution, though less pharmacological flexibility. The fastest time to peak current in our recordings was approximately 75 ms (for 1 mM GABA applications), approaching the rate of solution change. This was far slower than the maximal rise time of 0.5 ms for GABA concentrations of 1–10 mM observed by Twyman [29], using an ultrafast ligand exchange system (exchange time of 0.1 ms) and mouse cortical neuron patches containing 5–25 channels (though at low GABA concentrations, the rise time was about 2 s, similar to our results). Similarly, using outside-out patches Maconochie and Knight [20] observed a rise time of 0.4 ms, and Jones and Westbrook [12] measured fastest rise times of about 1.8 ms, while Puia et al. [25] observed the fastest time to peak, of the order of 0.4 ms in nucleated patches from cerebellar granule neurons. However, Gingrich et al. [8], using a two-barrel control/GABA pipette system with solution change within 1–2 ms, recorded a fastest time to peak of 30 ms with 1 mM GABA application for both α1 β2 γ2S and α3 β2 γ2s receptors in whole-cell recordings. The maximal rate of rise of GABA currents is

thus not only a function of the solution exchange rate, but depends heavily on the recording technique (whole-cell versus single-channel or macropatch). The slower time to peak in whole-cell recordings compared with that seen in isolated membrane patch recordings is probably related to the sequential activation of spatially distributed channels and the delays in diffusion associated with cell adherence to the dish. The wavefront of drug solution moving at 10 cm/s over a cell of 50 μm diameter will take at least 0.5 ms to wash over the cell, not accounting for areas where diffusion is more limited. For patch recording, the number and spatial distribution of channels are far smaller, and solution exchange rate becomes more critical. Maconochie and Knight [20] have calculated the theoretical limit to the speed of solution change (based on diffusion calculations) to be approximately 0.2 ms, which may be the limiting factor for high concentration applications to excised patches. At low GABA concentrations and whole-cell recordings, results with the multipuffer system and ultrarapid techniques are quite similar. While the speed of multipuffer application is insuffficient for ultrarapid kinetic studies of GABAR-containing macropatches or single channels, it appears to be fast enough for meaningful whole-cell pharmacology at GABA concentrations below 300–1000 μM as well as "steady-state" single-channel recordings.

The time course for GABAR current development in our experiments could be modeled as the sum of two exponential association functions. The time constant for current development should be a complex function of the association and dissociation rates for GABA, the rate of channel opening after binding of GABA, and the rates of exit to desensitized states. Although prior models from our laboratory based on single-channel burst kinetic data have included two GABA-binding steps and distal closed states to model intraburst closures [19, 31], the simplest associated model that takes into account the binding of ligand to receptor and subsequent opening of the liganded channel takes the following form:

$$R + A \underset{k_{-1}}{\overset{k_1}{\Leftrightarrow}} RA \Leftrightarrow RA^*$$

where R refers to the receptor, A to agonist (GABA), RA to the liganded receptor and RA^* to the open conformation of the channel (assuming, for the moment, a single binding site, a single open state, and no desensitized states [11]). Assuming further that channel opening rate is fast relative to binding, the time course of current activation will be a function primarily of the binding rate, given by the equation $I(t) = A\,(1–\exp(\{(k_1[A] + k_{-1})t\})$. The dissociation rate, k_{-1}, can be inferred from the dissociation constant for the complex at equilibrium, which is determined empirically from the observed EC_{50} (12.2 μM). While the true activation constants cannot be determined from the data available, activation rates consistent with the observed activation coefficient of 1.14×10^5 M^{-1} s^{-1} and K_d of 12.2 μM could be modeled with a relatively slow off-rate, k_{-1}, of 1.5 s^{-1} and an association rate, k_1, of 1.23×10^5 M^{-1} s^{-1}. These numbers are approximately tenfold slower than those used in other recent kinetic models [5, 8, 21, 29]. Gingrich et al. [8] were able to account for the activation and desensitization rates observed to occur in whole-cell currents using a two binding site gating model developed in our laboratory to account for intraburst and extraburst neuronal single-channel kinetic properties, with whole-cell simulated currents first-order filtered at 12 Hz (–3 db) to account for the limitations of the response time. They found that different α subunit subtypes resulted in marked differences in channel activation rates at the whole-cell level, and modeled the α1-containing-receptors with an on-rate (k_1) of 2.1×10^6 M^{-1} s^{-1} and off rate (k_{-1}) of 14.6 s^{-1}, or a tenfold faster off rate and 20-fold faster on-rate. Celentano and Wong [5] obtained the best fit to their data with an on-rate (k_1) of 2.97×10^6 M^{-1} s^{-1} and an off-rate (k-$_1$) of 43.1 s^{-1}, though their measured off-rate with a time constant of 230 ms predicted a dissociation time constant of 4.35 s^{-1}. Both Maconochie et al. [21] and Twyman [29], while not proposing specific rate constants, found a maximum channel opening rate of 6000 to 6500 s^{-1}. The most likely explanation for the slower activation rates seen in our recordings is the "low-pass filtering" resulting from the rate of solution application and recording in whole-cell configuration, as noted by Gingrich et al. [8]. However, it should be stressed that meaningful rate constants cannot be obtained from whole-cell recordings with the solution exchange rates observed with multipuffer application.

We observed concentration-dependent desensitization of GABAR currents in the continued presence of agonist, which could be modeled with a single exponential decay with time constants ranging from 4.3 s for 1 mM to almost 300 s for 10 μM GABA. These time constants were similar to those observed by Frosch et al. [7] using single "puffer" micropipette application onto cortical neurons in culture, and the desensitization rates observed by Gingrich et al. [8] with a rapid application system onto transfected HEK293 cells (though they did not model these rates with exponential functions per se). Several laboratories [5, 12, 21], using ultrarapid (submillisecond) application systems onto macropatches, have demonstrated rapid phases of desensitization of GABAR currents with exponential decay time constants of the order of 10–20 ms, which might not be detected by multipuffer application. Celentano and Wong [5], using a multibarrel application system with solution change in under 1.5 ms to apply GABA solutions to outside-out macropatches, noted three phases of desensitization with time constants of 15.4, 207 and 1370 ms. However, these rapidly desensitizing states become prominent only at very high GABA concentrations (300 μM to 1 mM [5]), and were not seen at the linear portion of the concentration/response curve, where much of the allosteric pharmacology of the receptor occurs [18, 26]. Moreover, the fastest τ for desensitization only comprised 15% of the desensitization at 300 μM and 20% at 1 mM. We did not observe the rapid phases of desensitization (with time constants of the order of tens to hundreds of milliseconds)

seen with ultrarapid drug application techniques and macropatch recording [5, 12]. In our whole-cell recordings, we have sometimes noticed a diminution of current peak amplitude at supramaximal GABA concentrations (producing a "U-shaped" concentration/response relationship, data not shown). In these cases, subsequent applications of lower concentrations of GABA produced smaller responses, implying that desensitization of some of the receptors had occurred. Application of high concentrations of GABA may accelerate transitions to a desensitized state from which recovery is slow, of the order of minutes. This desensitization of the response presumably occurred during the time of solution equilibration (i.e., the first 50–100 ms of application), before the peak current was expressed. This would be consistent with a desensitization time constant shorter than 100 ms. Celentano and Wong [5] noted that preapplication of 30 μM GABA eliminated the fast phase of current desensitization, blunting the response, while a brief wash after completion of the rapid phase of desensitization (to 1 mM GABA) again decayed with biphasic kinetics, consistent with the remaining (non-desensitized) receptors being capable of interconversion between desensitized states. Although rapid desensitization rates (and the associated transient peaks currents) might have been obscured in our system by the relatively slower rate of drug onset (10–90% rise time of 54 ms), the GABARs that desensitized prior to channel opening are thus part of the same population of channels that subsequently open and desensitize more slowly. While the major effect of this "lost phase" of desensitization is a blunting of currents elicited by higher concentrations of GABA, resulting in a modest leftward shift of the EC_{50} [5], the basic pharmacology of the receptor and the kinetics of currents elicited by lower concentrations of GABA are not different from those seen with ultrarapid techniques and macropatch recording. Ultrarapid application systems are important for evaluating the kinetics of GABAR opening and desensitization in single-channel or multichannel patch recordings at high GABA concentrations, simulating conditions that may occur at some inhibitory synapses [6].

The multipuffer is a device for applying limited quantities of drug solutions rapidly to small areas of a cell culture dish for use in electrophysiological recordings. Unmodified U-tube techniques and multibarrel large-diameter (200 μm) pipette applications (e.g., Celentano and Wong [5]) used for ultrarapid drug application allow many drugs to be used during the course of an experiment, but bathe the entire culture dish with drug solution, potentially leading to desensitization of receptors on other cells and necessitating another source of saline superfusion and an additional drain for the drug to be removed from the medium. Glass micropipette "puffers" or multibarrel pipettes pulled to a fine tip (10–20 μm) can apply small amounts of a single drug concentration per pipette barrel to restricted areas of the culture dish. These techniques are excellent for applying small volumes of precious reagents (e.g., enzymes or rare/expensive drugs). However, each drug concentration comes from a puffer pipette located at a different angle to the cell/patch from which recordings are being made, or from an opening of different size and position on a multibarrel pipette, hence the response times and delays cannot be identical. The multipuffer device allows: (1) close proximity to the cell of interest (within 50–100 μm), without obscuring the visual field, (2) brief applications of small volumes, minimizing desensitization of receptors on other cells, (3) a relatively rapid rate of application, and (4) suction of drug solutions back into the tip after application due to the Bernoulli effect, without need of an additional drain or superfusion. In addition: (1) the pipette tip can remain close to the cell or patch throughout the recording, (2) the rate of solution application can be controlled by adjusting the height of the drug reservoirs and the micropipette tip diameter, (3) new drug solutions can be mixed and used immediately, and (4) the system is relatively simple, low in cost and easy to use and maintain.

Limitations of the multipuffer device include: (1) it is not suitable for "precious" reagents (enzymes, etc.) that cannot be prepared in large volumes for dilute application, (2) "layered" drug application (i.e., preapplication of one drug or concentration followed immediately by a second drug or a combination of two drugs) would require a second multipuffer, and (3) it is not suitable for studies of receptors or channels that require applications on a submillisecond time scale. Other practical problems include bubbles in the tubing, leakage of air or drug solutions, and plugging of the glass pipette tip, particularly in recording solutions with a lot of cellular debris, though this may be minimized by positive perfusion with recording saline during periods between drug applications.

Acknowledgements We thank Merlin Fox and the Instrument Shop of the Dept. of Physiology, University of Michigan, for assistance in development and manufacture of the multipuffer device. We also thank Dr. Martin Chalfie for providing the cDNA encoding green fluorescent protein, and Fang Sun for subcloning *gfp* into pCMVneo. L.J.G. was supported by a Clinical Investigator Development Award (NIH K08 NS01652) and a Neuropharmacology Fellowship from the American Academy of Neurology. This study was supported by R01-NS33300 (RLM).

References

1. Angelotti TP, Macdonald RL (1993) Assembly of $GABA_A$ receptor subunits: $\alpha_1\beta_1$ and $\alpha_1\beta_1\gamma_{2S}$ subunits produce unique ion channels with dissimilar single-channel properties. J Neurosci 13:1429–1440
2. Angelotti TP, Uhler MD, Macdonald RL (1993) Assembly of $GABA_A$ receptor subunits: analysis of transient single-cell expression utilizing a fluorescent substrate/marker gene technique. J Neurosci 13:1418–1428
3. Betz H (1990) Ligand-gated ion channels in the brain: the amino acid receptor superfamily. Neuron 5:383–392
4. Burgard EC, Tietz EI, Neelands TR, Macdonald RL (1996) Properties of recombinant $GABA_A$ receptor isoforms containing the α5 subunit subtype. Mol Pharmacol 5:119–127
5. Celentano JJ, Wong RKS (1994) Multiphasic desensitization of the GABA(A) receptor in outside-out patches. Biophys J 66:1039–1050

6. Dekoninck Y, Mody I (1994) Noise analysis of miniature IPSCs in adult rat brain slices – properties and modulation of synaptic GABA(A) receptor channels. J Neurophysiol 71:1318–1335
7. Frosch MP, Lipton SA, Dichter MA (1992) Desensitization of GABA-activated currents and channels in cultured cortical neurons. J Neurosci 12:3042–3053
8. Gingrich KJ, Roberts WA, Kass RS (1995) Dependence of the $GABA_A$ receptor gating kinetics on the α-subunit isoform: implications for structure-function relations and synaptic transmission. J Physiol (Lond) 489:529–543
9. Greenfield LJ, Uhler MD, Macdonald RL (1994) Cyclic GMP-dependent protein kinase II regulates recombinant $GABA_A$ receptor currents in L929 cells (abstract). Soc Neurosci Abstr 20:503
10. Hamill OP, Marty A, Neher E, Sakmann B, Sigworth FJ (1981) Improved patch-clamp techniques for high-resolution current recording from cells and cell-free membrane patches. Pflugers Arch 391:85–100
11. Hille B (1992): Ionic channels of excitable membranes, 2nd edn. Sinauer, Sunderland, Mass., pp 146–158
12. Jones MV, Westbrook GL (1995) Desensitized states prolong $GABA_A$ channel responses to brief agonist pulses. Neuron 15:181–191
13. Kapur J, Macdonald RL (1996) Pharmacological properties of $GABA_A$ receptors from acutely dissociated rat dentate granule cells. Mol Pharmacol (in press)
14. Kume A, Greenfield LJJ, Macdonald RL, Albin RL (1996) Felbamate inhibits [^{3}H]t-butylbicycloorthobenzoate binding and enhances Cl^- current at the gamma-aminobutyric $acid_A$ receptor. J Pharmacol Exp Ther 277:1784–1792
15. Lin Y, Angelotti TP, Dudek EM, Browning MD, Macdonald RL (1996) Enhancement of recombinant α1β1γ2L $GABA_A$ receptor whole cell currents by protein kinase C is mediated by phosphorylation of both β1 and γ2L subunits. Mol Pharmacol 50:185–195
16. Lin Y, Browning MD, Dudek EM, Macdonald RL (1994) Protein kinase C enhances recombinant bovine α1β1γ2L $GABA_A$ receptor whole-cell currents expressed in L929 fibroblasts. Neuron 13:1421–1431
17. Macdonald RL, Olsen RW (1994) $GABA_A$ receptor channels. Annu Rev Neurosci 17:569–602
18. Macdonald RL, Weddle MG, Gross RA (1986) Benzodiazepine, beta-carboline, and barbiturate actions on GABA responses. Adv Biochem Psychopharmacol 41:67–78
19. Macdonald RL, Rogers CJ, Twyman RE (1989) Kinetic properties of the $GABA_A$ receptor main conductance state of mouse spinal cord neurones in culture. J Physiol (Lond) 410: 479–499
20. Maconochie DJ, Knight DE (1994) A method for making solution changes in the sub-millisecond range at the tip of a patch pipette. Pflügers Arch 414:589–596
21. Maconochie DJ, Zempel JM, Steinbach JH (1994) How quickly can GABA(A) receptors open? Neuron 12:61–71
22. Murase K, Ryu PD, Randic M (1989) Excitatory and inhibitory amino acids and peptide-induced responses in acutely isolated rat spinal dorsal horn neurons. Neurosci Lett 103:56–63
23. Newland CF, Cull-Candy SG (1992) On the mechanism of action of picrotoxin on GABA receptor channels in dissociated sympathetic neurones of the rat. J Physiol (Lond) 447:191–213
24. Porter NM, Angelotti TP, Twyman RE, Macdonald RL (1992) Kinetic properties of alpha 1 beta 1 gamma-aminobutyric $acid_A$ receptor channels expressed in Chinese Hamster Ovary cells: regulation by pentobarbital and picrotoxin. Mol Pharmacol 42:872–881
25. Puia G, Costa E, Vicini S (1994) Functional diversity of GABA-activated Cl^- currents in purkinje versus granule neurons in rat cerebellar slices. Neuron 12:117–126
26. Rogers CJ, Twyman RE, Macdonald RL (1994) Benzodiazepine and beta-carboline regulation of single GABA(A) receptor channels of mouse spinal neurones in culture. J Physiol (Lond) 475:69–82
27. Saxena NC, Macdonald RL (1994) Assembly of $GABA_A$ receptor subunits: role of the delta subunit. J Neurosci 14:7077–7086
28. Schofield PR, Darlison MG, Fujita N, Burt DR, Stephenson FA, Rodriguez H, Rhee LM, Ramachandran J, Reale V, Glencorse TA (1987) Sequence and functional expression of the GABA-A receptor shows a ligand-gated receptor super-family. Nature 328:221–227
29. Twyman RE (1994) GABA-A receptor channel opening rates in excised patches of mouse cortical neurons. Jpn J Physiol 44:S87-S90
30. Twyman RE, Rogers CJ, Macdonald RL (1989) Pentobarbital and picrotoxin have reciprocal actions on single $GABA_A$ receptor channels. Neurosci Lett 96:89–95
31. Twyman RE, Rogers CJ, Macdonald RL (1990) Intraburst kinetic properties of the $GABA_A$ receptor main conductance state of mouse spinal cord neurones in culture. J Physiol (Lond) 423:193–220